# Mission Design and Analysis of USM High-Altitude Balloon

*Ahmad Shaqeer Mohamed Thaheer*
*Norilmi Amilia Ismail*
*School of Aerospace Engineering, Engineering Campus, Universiti Sains Malaysia, 14300, Nibong Tebal, Pulau Pinang, Malaysia*

## ABSTRACT

*High-altitude balloons (HABs) are unmanned balloons, which are usually filled with helium or hydrogen and can float over approximately 50 km above the sea level. This study aims to develop the mission planner and hardware associated with HAB. The main system of HAB is divided into five subsystems, namely, balloon and navigation, communication, on-board data handling and payload, structure, and thermal system. The design process starts by determining the mission requirements. Through the mission timeline, the flight time is estimated to configure the mode of operation for the mission. A tradeoff analysis is conducted on selected components. The initial selected components that are suitable for the mission are tested individually based on several case studies. After the component testing, the subsystems are integrated and are tested as a whole system. Based on the preliminary results, the configuration and design of the HAB is finalized and a test launch is performed. Finally, the flight test results are collected and analyzed.*

## Introduction

High-altitude balloons (HABs) are unmanned balloons, which are usually filled with helium or hydrogen and can float over approximately 50 km above the sea level. A HAB is usually used as a weather balloon [1] for obtaining weather conditions, such as temperature and pressure throughout the flight course. The extreme condition in the stratosphere can plunge to as low as −56.5 °C in temperature and 2 kPa in pressure [2]. Other HAB applications include a platform for stratospheric exploration and research [3–5]. Google X introduced Project Loon, which uses HABs to provide Internet access to remote areas [6]. The project also has a potential for space tourism; specifically, a private company in the United States named World View has proposed a passenger-carrying capsule to be lifted up to the stratosphere and descend back to Earth using a parafoil attached to the capsule [7].

HABs have attracted the public interest in recent years with large number of HAB projects being released into the stratosphere due to the advancement in low-cost communication technology and easy accessibility to civilian global positioning systems (GPSs). Such a project is an effective alternative to satellite in terms of providing the same application and has better cost benefit as it uses green technology by replacing the use of conventional rocket to send satellites into space. The payload carried by HAB is also retrievable, thereby providing opportunity for service and maintenance and reducing space debris.

### Concept of Operations

A typical HAB is operated by attaching a helium-filled balloon with a payload bus that contains atmospheric sensors (e.g., temperature, pressure, and humidity sensors) and a camera to record the scenic view of the Earth's curvature. A small parachute is attached between the payload bus and the balloon as shown in Figure 1. The parachute functions to slow down the payload bus during descent and thus facilitate safety landing.

Thereafter, the balloon is released and ascends to the stratosphere. During its ascent, the pressure of the external environment is lower than the pressure inside the balloon. Given the pressure difference, the balloon will start to expand up to a point at which the balloon can no longer withstand the internal pressure and will therefore burst. The bursting of the balloon indicates that the maximum altitude is achieved during the flight.

After bursting, the parachute will deploy and slow down the descent of the payload bus. The parachute will initially not deploy completely due to low air density at high altitude; however, as it descends and the air density increases, the parachute will eventually fully deploy. The path of the descended payload is significantly affected by the wind in the absence of parachute control. Thus, trajectory prediction is important prior to launching

the HAB. Finally, the search and rescue team can retrieve the payload, and the data saved on-board can be further analyzed. The summary of the operation is illustrated in Figure 2.
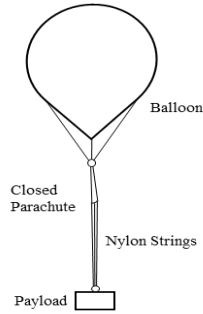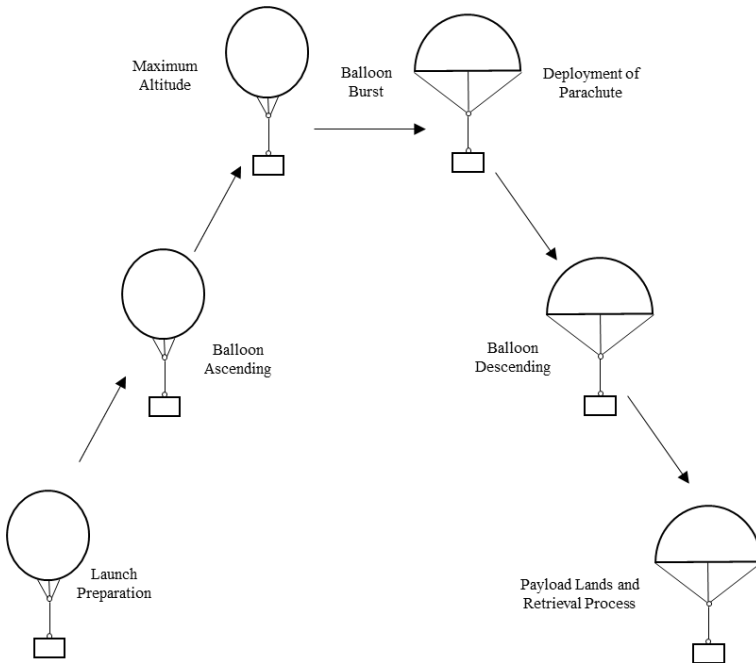


Figure 1: HAB configuration



Figure 2: Concept of HAB operation

## Mission Design

### Mission Objective
The current project aims to collect atmospheric data and capture images of the Earth's horizon. Accordingly, interest on spacecraft design can be facilitated among undergraduate students.

### Mission Timeline
The preliminary operational timeline of the experiment is illustrated in Figure 3.

**Prior to Launch: (T=-2)**
All required considerable equipment is ready and all subsystems have undergone final inspection

**Launch Preparation: (T=-1)**
Inflation of the balloon

**Launch: (T=0)**
Launching of the balloon

**Waiting Time: (T=0.5)**
Ascending of the balloon in altitude with blocked telemetry

**Live Feed: (T=0.1)**
Turn on live feed communication

**Preliminary Tracking: (T=1)**
Preliminary tracking to predict the trajectory

**Rescue: (T=1.1)**
Tracking team is dispatched based on preliminary tracking

**Live Feed: (T=2.5)**
Recommencing of live feed communication

**Balloon Burst Time: (T=2.1)**
Estimation of balloon bursting time

**Rescue Team Update: (T=2.51)**
Tracking team location update

**Payload Retrieval: (T=2.87)**
Payload retrieval after landing

**Data Processing: (T=24)**
Analysis of data, including images, videos, and temperature reading
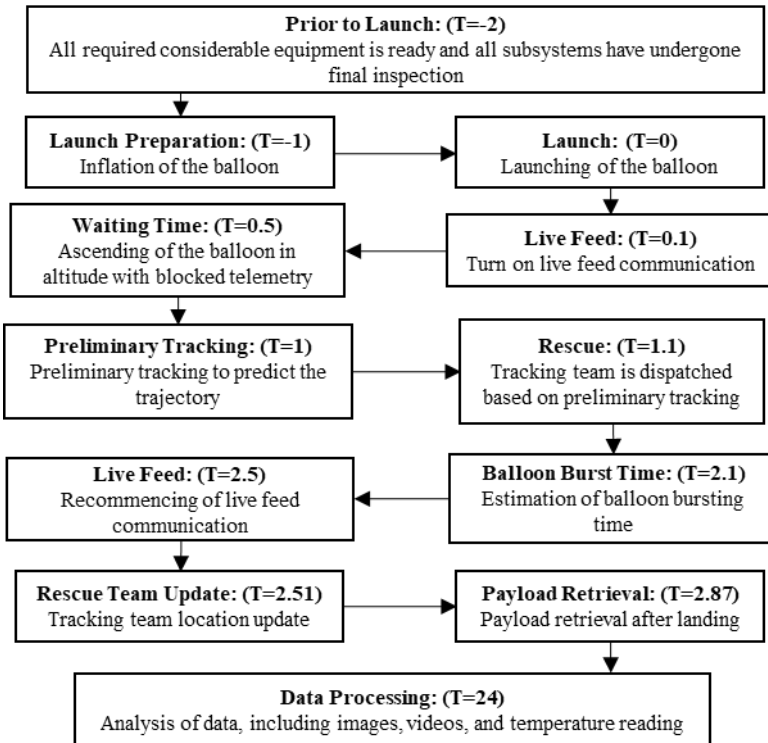
Figure 3: Mission timeline

## System Overview

System integration is vital to ensure that the mission is successful and meets all the objectives. The overall system design of HAB can be divided into five subsystems, namely, balloon and navigation, communication, on-board data handling (OBDH) and payload, structure or bus, and thermal subsystems. The payload bus is made of polystyrene (30 cm × 30 cm × 30 cm), which is lightweight, waterproof, and capable of floating. Inside the bus, the components are stacked. In particular, the power supply is placed at the bottom level, OBDH and payload are placed in the middle level, and the communication systems are placed on the top level of the stack. The heat packs are placed at the bottom of each stack plate. Temperature and humidity sensors as well as the antenna are positioned outside of the box for improved functionality. The payload is then connected with a parachute and tied to the balloon line.

The balloon trajectory can be predicted using software programs. The flight prediction software programs developed by the University of Cambridge [8] and University of Wyoming [9] are widely used by balloon hobbyists in predicting the path and landing area of balloons. The two software programs consider the weather forecasts, including wind direction and magnitude, from the meteorological department. The simulation accuracy is generally high when the estimated date is close to the launch date of the balloon.

A communication subsystem is necessary to track the balloon location. The core components of such subsystem are the transmitter located on the HAB and the receiver located on the ground [10]. The communication subsystem works closely with the OBDH in tracking the balloon trajectory during flight. In summary, OBDH acts as the brain of the mission by controlling all on-board sensors and payload, as well as the communication subsystem.

The payload is contained in a structure that protects it from harsh thermal conditions at high altitudes and high impacts during landing. The payload is kept warm under different atmospheric conditions by use of a thermal subsystem unit. In this case, the thermal subsystem needs to ensure that the temperature in the bus is well regulated and maintained at the optimum temperature for the on-board system to function and perform perfectly.

The main function of each subsystem is presented in Figure 4. The critical subsystems are the OBDH and payload, and communication subsystem. However, other subsystems are of equal importance depending on the mission objective. The design process includes a risk analysis for all subsystems.

The two subsystems mentioned above should be thoroughly tested and verified prior to launching to avoid mission failure. In the current project, six

tests are conducted, including one integration test, to ensure reliability, capability, performance, and efficiency of components in various conditions. The risks associated with these subsystems are identified, and the management plan for the risks is developed.
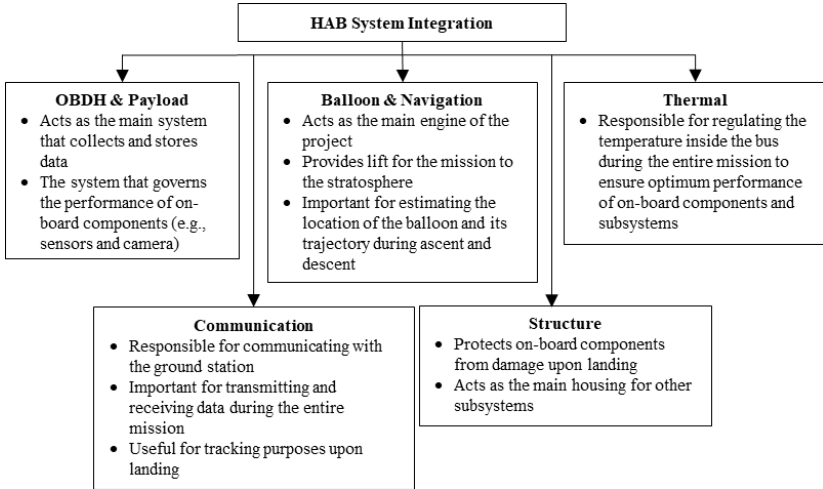


Figure 4: HAB system integration

# Hardware Design

## Communication Subsystem

The communication subsystem aims to track the HAB during its flight. Data are transmitted one-way from the balloon to the ground station. No active payloads on-board require commands in other directions (i.e., from ground to the balloon). The objective can be achieved through the two paths illustrated in Figure 5.
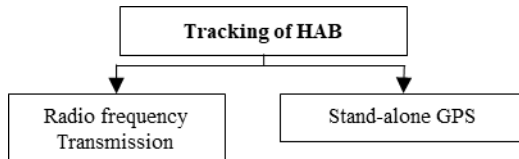


Figure 5: Tracking method of HAB

The radio frequency (RF) transmission path is the primary tracking mode for the present mission. The general communication subsystem architecture is shown in Figure 6. The communication range is between 10 and 30 km, depending on the highest altitude achieved by the HAB. The HAB carries a GPS receiver, transmitter, and an antenna module, while the ground station is equipped with a receiver and an antenna unit. The altitude, longitude, and latitude are transmitted to the ground station to track the balloon location. These data are obtained from the on-board GPS receiver that triangulates its current position by simultaneously tracking its position relative to several satellites. This information is then relayed to the transmitter through an on-board microcontroller and is transmitted to the ground station through the antenna.

The transmitter and antenna on the HAB as well as the receiver and antenna at the ground station must be at the same frequency and protocol. When the receiver at the ground station receives the transmission from the HAB, the data are decoded and read directly through a computer.
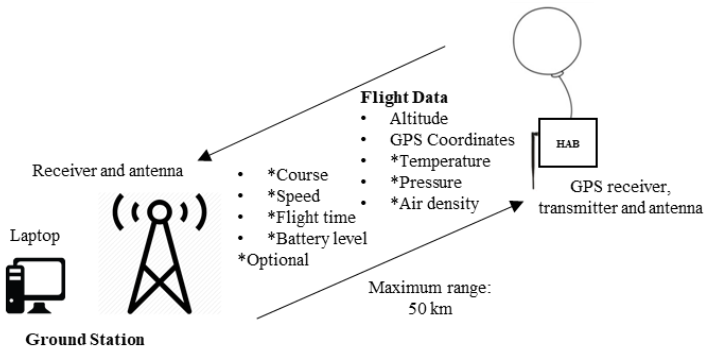


Figure 6: General architecture of the communication subsystem

RF Transmission

The local amateur radio (also called the ham radio network coverage) offers an extremely wide horizontal range of coverage and helps the balloon detection during ascent and descent. A custom-made Arduino shield called Trackuino is used to transmit data from the HAB. Trackuino consists of a transmitter, GPS receiver, audio beeper, and sensors. The system architecture of Trackuino is shown in Figure 7. Trackuino transmits the flight data in the form of Automatic Packet Reporting System (APRS) packet data. These

APRS packet data can be readily received by radios and relayed around by digipeaters before the data are passed to the Internet through an IGate. The data are sent to a website called aprs.fi, wherein the live flight path of the balloon can be viewed. The manual, schematics, and firmware for the Trackuino shield are open source and widely available online.

The disadvantage in using Trackuino transmitter is the limited tracking distance of only up to 10 km. This condition raises the possibility of the balloon to deviate from its simulated flight path at altitudes above 10 km without the knowledge of the ground station. However, the possibility of clear line-of-sight and less dense air in the sky can increase the transmission range [11]. The balloon recovery outside of its simulated flight path can also be resolved by the wide network of the amateur radio.
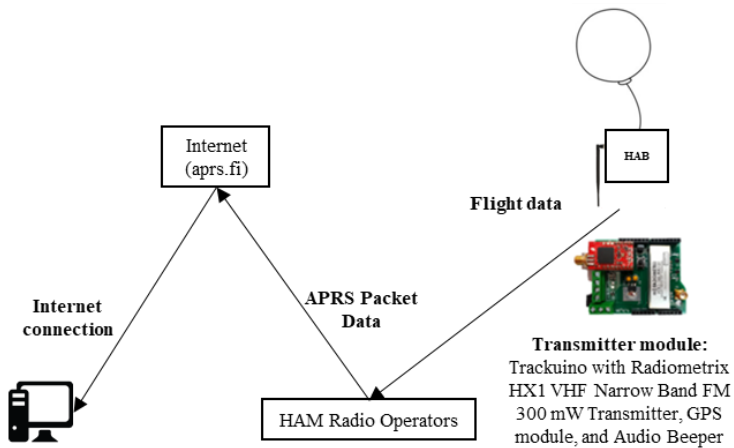


Figure 7: Trackuino system architecture for HAB tracking

The communication subsystem uses HX1 shown in Figure 8(a). The transmitter is a narrow band radio type that offers an RF output of 300 mW and a very high frequency data link that is suitable for long range data transfer and low power applications unlike current transmitters.

## Stand-alone GPS

The stand-alone GPS is treated as a secondary mode of tracking or a redundant system. A SPOT Satellite GPS Messenger shown in Figure 8(b) is used as a stand-alone GPS system in this study. Given its limited altitude coverage of only up to 7 km, the system only functions to detect the balloon location during landing.
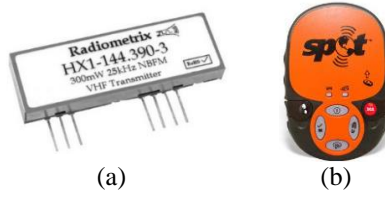
(a)                         (b)

Figure 8: (a) HX1 144.39 MHz transmitter module [12]. (b) SPOT Satellite GPS Messenger [13]

Antenna

The selected antenna for the system is a monopole rubber ducky antenna. It consists of a wire in a narrow helix shape and sealed in a rubber or plastic jacket. Similar to the one-fourth wave ground-plane antenna, the size of the antenna needs to suit the frequency of the waves that it transmits. However, the size required is very small relative to the size required for the one-fourth wave ground-plane antenna. Considering the size constraint for performance, the rubber ducky antenna is suitable to the project.

## OBDH and Payload

The On-board Data Handling (OBDH) subsystem of the HAB uses a microcontroller to connect each sensor and the payload according to their own requirement. The memory and processor store the command and regulate the action needed for each component through the output peripherals.

The microcontroller used for the HAB mission is Arduino Uno. The subsystem also includes power management, which depends on the specification of the available power supply. The power supply generally comes from batteries due to their limited bus size. Thus, few criteria must be considered in battery selection, such as weight, discharge rate at critical temperature and pressure, voltage supply, and current. The selection is determined through the total power consumption based on the Equation (1):

$$Q = I \cdot t = \frac{P \cdot t}{V} \tag{1}$$

where $P$ is the total power consumption in mW, $V$ is the voltage of the battery in voltage, $I$ is the current in ampere, $Q$ is the charge of the battery in mAh, and $t$ is the operating time in hour.

The calculation is based on the assumptions that no power losses are generated at the voltage regulator and in the circuit, the battery can operate in

extreme temperature, and the estimated power safety factor is only 50%. A voltage regulator is needed to maintain a constant voltage as each component has different power requirements. The design may be as simple as feed-forward design, or may include negative feedback control loops. An electromechanical mechanism, or electronic components may also be used to regulate one or more AC or DC voltage.

In the HAB operation, the communication occurs only between the HAB and the ground station in a limited time. Most data are stored in the memory card, thereby decreasing data transfer. The microcontroller can tune the transmitter to work only for the communication subsystem and ultimately reduce data loss during transmission.

## Microcontroller

The selected microcontroller for the mission is Arduino due to its simplicity, lightweight, and wide range of resources. Arduino Uno is a microcontroller board based on ATmega328.
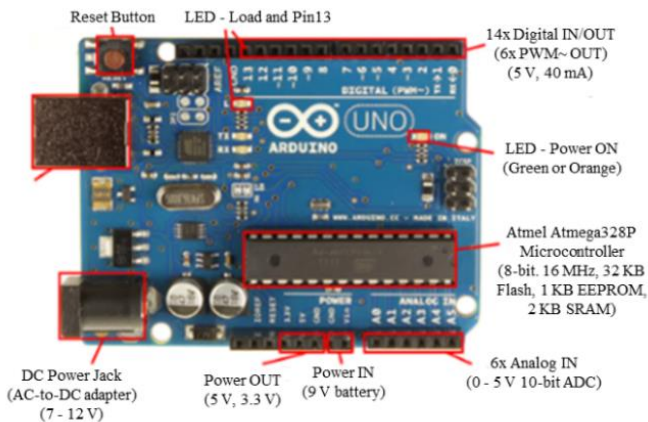
Figure 9: Arduino pin assignment [14]

As shown in Figure 9, Arduino has 14 digital input or output pins, 6 analogue inputs, a 16 MHz ceramic resonator, a USB connection, a power jack, an ICSP header, and a reset button. The microcontroller obtains all necessary supports by simply connecting it to a computer with a USB cable or by powering it with an AC-to-DC adapter or even battery. The adapter can be connected by plugging in a 2.1 mm center-positive plug into the board power jack. The board can operate with an external power supply of 6–20 V. If the power supply is less than 7 V, then the 5 V pin may supply less than 5 V and

the board may be unstable. If more than 12 V is used, then the voltage regulator may overheat and the board may be damaged. Therefore, the recommended power supply range is 7–12 V. Uno differs from all preceding boards because it does not use the FTDI USB-to-serial driver chip but features the Atmega16U2 programmed as a USB-to-serial converter.

## Sensors

BMP180 is a sensor that is designed specifically for measuring barometric pressure and temperature. It is the next-generation sensor from Bosch and replaces the old BMP085. The sensor is completely identical to BMP085 in terms of firmware, software, and interfacing, and works well with the example code from the previous version. The sensor is soldered to a PCB with a 3.3 V regulator, $I^2C$ level shifter, and pull-up resistors on the $I^2C$ pins. The connections between the sensors to Arduino are easy; the VIN pin is simply connected to the 5 V voltage pin, GND to ground, SCL to $I^2C$ Clock (Analogue 5), and SDA to $I^2C$ Data (Analogue 4).

## Camera

Action cameras are used to capture videos throughout the mission due to their capability to capture high-definition videos in wide-angle view. The cameras are also lightweight and small and are thus perfect for a HAB mission that requires compact subsystems.

## Power

Lithium AA batteries are more suitable to the current project than other commercial off-the-shelf products because of the high-power output, compatible temperature range, and low weight of the former.

## Structure Subsystem

The main structure is important as it ensures that all components are well placed and fixed even if the bus becomes unstable during flight. The structure should have high strength-to-weight ratio, high buoyancy, and good resistance to any high impact during landing.

The shape plays an important role in maintaining the HAB stability. A cube shape of large contact area produces rotating motion as a result of high wind speed but is easy for component placement and access for maintenance. A cylindrical shape produces less rotation but is difficult for subsystem placement. The velocity of the HAB will significantly drop during descending as its weight is light. Therefore, a blunt shape bus helps in increasing drag, thereby reducing the descent rate and saving the payload from experiencing a high impact during landing.

Material selection affects the weight of the structure. Metal structure proves to be heavy yet strong, while polystyrene is light but low in strength.

However, polystyrene is ideal because it can float in water and can be easily carved and shaped. The size of the bus can be determined by solving the pressure exerted on the bus. The total weight of the bus is calculated by using Equation (2):

$$W_{Total} = W_{Payload} + W_{Bus} + W_{Comm.} + W_{Thermal} + W_{Parachute} \qquad (2)$$

Then, the pressure is calculated by assuming that the force is equal to the weight. Low pressure is ideal as it shows that low force is acting on the bus. Finally, other materials, such as adhesives or impact absorbers, can be used to ascertain improved and complete main structure.

A stack and compartment concept is developed for the inner payload arrangement. Leaving the inner box with many empty spaces is undesirable as it contains many air particles, which will become a medium for the outside temperature to conduct easily inside the box and thus decreasing the temperature. The inner box is filled with the EPS foam that can be carved and shaped to solve the abovementioned problem. The foam is carved for each compartment such as for microcontroller, battery pack, and SPOT Messenger GPS. In this way, the components can be kept rigid in place to avoid movement during impact or spinning during flight. The heat pack is then attached on each side of the EPS foam to warm the payload components.
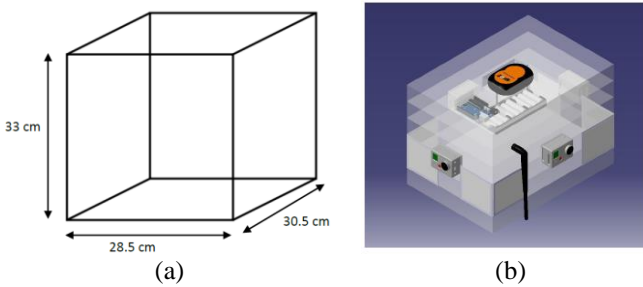


|     |     |
| --- | --- |
| (a) | (b) |

Figure 10: (a) Payload envelope size. (b) Payload stacked compartment concept

The camera is positioned at the highest point on the side of the box and tilted to 35° to capture an overall image of the horizon. The size is reduced to ensure rigidness of the payload box and to use a small working area shown in Figure 10(a). The total weight of the HAB can be calculated using Equation (2):

$$W_{Payload} = 230 \text{ g} \qquad W_{Bus} = 1400 \text{ g} \qquad W_{Comm.} = 347.4 \text{ g}$$

$$W_{Parachute} = 500 \text{ g} \qquad W_{Thermal} = 300 \text{ g}$$

Therefore, the total weight is 2777.4 g.

## Thermal Subsystem

The thermal system functions to ensure that the payload is operating at its optimum condition and temperature during its entire flight to the stratosphere and back to Earth. The data given by the meteorological department show that the temperature range between the sea level and an altitude of 20 km is between −60 and 30 °C. According to the payload specification, the operating temperature is from −40 °C to 85 °C. Thus, an efficient heating system should be designed to regulate the temperature inside the box. The time of flight relative to the altitude is considered in optimizing the thermal system performance. The calculation based on the ascent rate and the payload mass are tabulated in Table 1.

Table 1: Estimation of temperature change rate and ascent rate

| Atmospheric Level | Troposphere | Stratosphere |
|---|---|---|
| Temperature Change Rate | −8 °C/km | 1 °C/km |
| Ascent Rate (with payload of 1.5 kg) | 29.284 min. | 3.66 min. |

The increase in payload mass decreases the ascent rate, thereby resulting in long travelling time at certain atmospheric levels. Therefore, thermal protection is necessary when temperature decreases in the tropospheric level. In this condition, the cold temperature takes a long time to travel into the material and to reduce the internal temperature of the bus. Accordingly, the performance of other subsystems can be affected.

The heat released for each component can be calculated as follows [15]:

$$T_J - T_a = P \times \theta_{JA} \qquad (3)$$

where $P$ is the maximum power dissipation in watts, $T_J$ is the temperature of a junction on the device in °C, $T_a$ is the temperature of surrounding ambient air in °C, and $\theta_{JA}$ is the thermal resistance of the components from junction-to-ambient air.

The heat source for calculating the temperature released by the components is identified and tabulated in Table 2.

Table 2: Possible heat source of components

| Trackuino | |
|---|---|
| **Code** | **Descriptions** |
| REG1117 | Low-Dropout Positive Regulator |
| LM60 | Temperature Sensor |
| MC74VHC1GT125 | CMOS Logic Level Shifter |
| MC74VHC1GT125 | CMOS Logic Level Shifter |
| MC74VHC1GT125 | CMOS Logic Level Shifter |
| PMV20XN | N-channel MOSFET |
| Venus638FLPx | GPS Receiver |
| Radiometrix XH1-144.390-3 | Transmitter |
| **Arduino** | |
| **Code** | **Descriptions** |
| LMV358IDGKR | Op-Amp |
| LP2985-33DBVR | Low-Dropout Regulator |
| NCP1117ST50T3G | Low-Dropout Regulator |
| Atmega 16U2-MU | FTDI Converter |
| Atmega 328P-PU | Main M/C |

Using Equation (3) and by determining the electrical properties of each component, the total power dissipation is 18.52 W. Consequently, the average temperature difference is 15.17 °C.

The internal temperature of the polystyrene box should be maintained to suit the payload temperature range in the operational condition. Thus, heat packs are used to release heat inside the box. Thermal reflectors are also used to prevent heat loss in long duration flight. Heat packs are used as the heat generator and aluminum foil is used as the thermal reflector in the thermal subsystem as shown in Figure 11.



(a)                    (b)

Figure 11: (a) Heat pack. (b) Thermal reflector

## Balloon and Navigation Subsystem

Trajectory prediction of the balloon is essential to estimate its landing location and to carefully plan its flight and retrieval processes. The Cambridge University Spaceflight (CUSF) Landing Prediction by the University of Cambridge [8] and the Balloon Trajectory Forecasts by the University of Wyoming [9] are the two commonly used programs for the said task. Both prediction programs are developed based on the Global Forecast System model of National Oceanic and Atmospheric Administration. Figure 12 shows the user interface of the CUSF program.
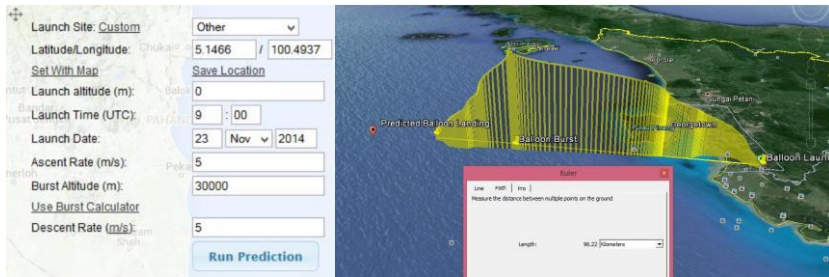


Figure 12: Input setting of CUSF landing predictor

Both softwares is limited in terms of prediction time. Specifically, the prediction of the landing location can only be simulated within 1 week or 180 h from the time of launch. The reason is that the weather can only be predicted within the available period.

Figure *13* shows the unavailability of the program when the input period is more than 180 h.



Figure 13: Unavailable prediction on December 16, 2014

The two software programs mentioned above confirm that the landing prediction in Figure 14 is considered accurate. The two software programs play an important role in the prediction of the HAB landing location with the established specific criteria.
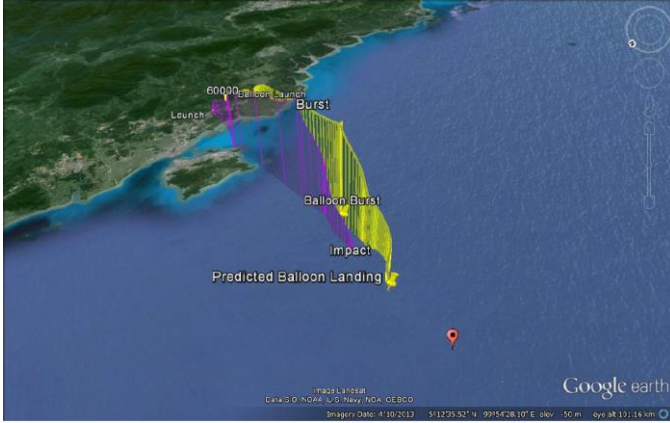


Figure 14: Predictions by CUSF and Balloon Track Program

The surrounding air density changes with temperature and pressure. The balloon is predicted to pass through three atmospheric layers of the Earth, which are troposphere (h < 11 km), first stratosphere (11 km < h < 20 km), and second stratosphere (20 km < h < 32 km) [16]. Considering that different regions have different air properties, the following equations are used to calculate air density at different atmospheric layers [16]. For the troposphere:

$$T = T_0 + L_{Trop.} h \tag{4}$$

$$P = P_0 \left( 1 + \frac{L_{Trop.} h}{T_0} \right)^{\frac{-gM}{RL_{Trop.}}} \tag{5}$$

For the first stratosphere:

$$T = 216.65 K \tag{6}$$

$$P = 22633 \cdot e^{\frac{-gM(h-11000)}{216.65R}} \tag{7}$$

For the second stratosphere:

$$T = 216.65 + L_{Strat.}\left(h - 20000\right) \tag{8}$$

$$P = 5475.2\left(\frac{216.65 + L_{Strat.}h}{216.65 + 20000L_{Strat.}}\right) \tag{9}$$

In the equations above, $T$ is the air temperature at the current altitude, $P$ is the air pressure at the current altitude, $T_0$ is the air temperature at sea level, $P_0$ is the air pressure at sea level, $L_{Trop}$ is the temperature lapse rate in the troposphere with a value of −0.0065 K/m, $L_{Strat}$ is the temperature lapse rate in the stratosphere with a value of 0.001 K/m, $g$ is the gravitational acceleration, $R$ is the universal gas constant with a value of 8.31447 J/mol·K, and $M$ is the molar mass of dry air.

To obtain the respective air density at different atmospheric layers, the following ideal gas equation is used:

$$\rho = \frac{PM}{RT} \tag{10}$$

The following equation can be used to estimate the diameter of the parachute:

$$D = \sqrt{\frac{8mg}{\pi\rho C_d v^2}} \tag{11}$$

A MATLAB® program for calculating the lift force, net lift force, bursting altitude, ascent rate, bursting time, and helium gas volume is created. The data in Figure 15 show the results for a payload mass estimated at 1.5 kg. The results are based on the assumptions that air density at sea level is 1.225 kg/m³, helium gas density at sea level is 0.179 kg/m³, the helium gas in the balloon has reached equilibrium in terms of pressure and temperature in ambient air, the change in density inside the balloon is equal to the change in density in the environment, and the balloon is ascending at a constant rate because the cross-sectional area of the balloon increases as the surrounding air density decreases.

The descent rate should not be higher than 5 ms⁻¹ to reduce the impact during landing. Figure 16 shows the drop velocity for four parachute

diameters. The drop velocity increases exponentially with the increase in altitude. At an altitude of 20 km, the drop velocity starts to show a constant pattern due to the constant density, which plays an important role in determining the drop velocity of a parachute as shown in Equation (11). The drop velocity is influenced by five parameters, namely, payload mass, gravitational acceleration, density of air, coefficient of drag, and diameter of parachute.
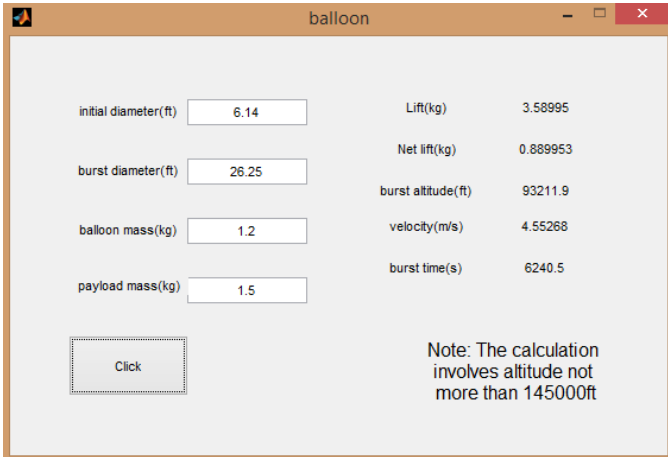


Figure 15: MATLAB® program for calculating the balloon parameters
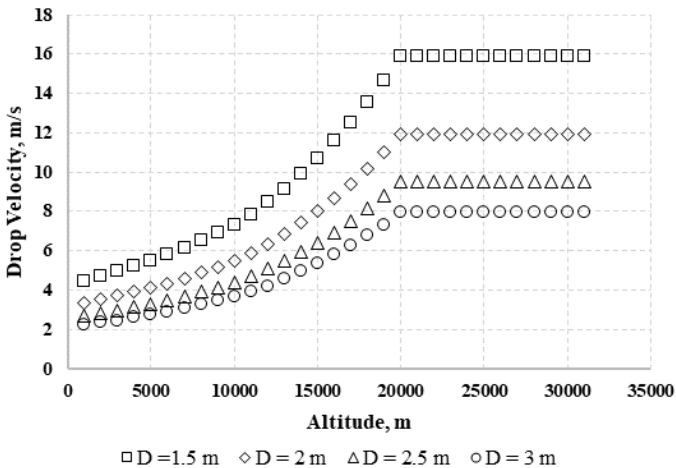
Figure 16: Graph of drop velocity against altitude

The landing prediction depends on the design of the parachute. The parachute reduces the descent rate and brings the payload safely by providing steady landing. The parachute must be lightweight, brightly colored, and be able to deploy automatically as it descends when the balloon has burst. A parachute has different types, including round, hexagonal, square, and Ram-air [17]. A round-shaped parachute is suitable to the project objectives as it provides pure drag unlike other types of parachutes. The said type can also sustain for a long time in the air.
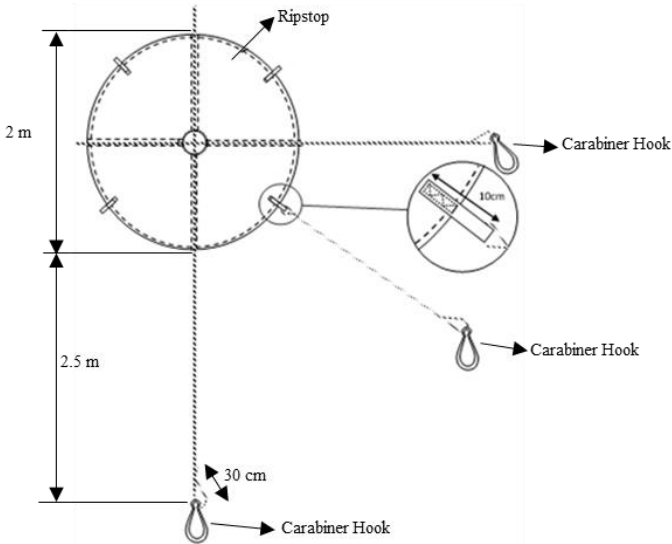


Figure 17: Parachute design

Figure 17 shows a spread-out configuration of the parachute design. The fabric of the parachute used is ripstop nylon fabric, which is water resistant and tear resistant. Ripstop nylon is woven with double or extra thick thread at regular intervals, thereby creating lattice patterns that prevent small tears from spreading. Bright color is selected for the parachute to standout without blending with the environmental colors while recovering the payload.

The diameter is determined to be 2 m to achieve a descent rate of 5 ms$^{-1}$. Nonetheless, during deployment testing with a load of 1 kg, the descent rate is found to be 2 ms$^{-1}$.

The paracord is sewed along the parachute, thereby forming two diagonal lines. In the middle of the parachute, an apex vent of 10 cm is cut out wherein the paracord crosses each other. In addition, a carabiner metal hook is used and linked to the balloon. The carabiner hook helps in reducing entanglement, which in turn reduces the HAB instability. Instability affects the video recording process, which can be handled by arranging the ropes inside the hook in favor of avoiding cross-over entanglements.

At the remaining four sides of the parachute, a hook using the same cloth is sewn on the four sides and nylon ropes is tied on the hook. The magnified illustration in Figure 18 shows that the hook is sewn securely with zigzag stitches. The ropes are tied to the hook using two half-hitch knots, and a zigzag line is stitched on the main rope.
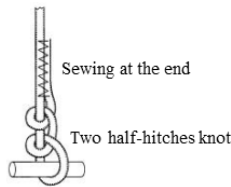


Figure 18: Two half-hitch knots and sewing at the ends

Helium gas is pumped into the balloon to create sufficient lift and thus bring the payload to 30 km (10000 ft.) above the sea level. The balloon used is PAWAN 1200. Table 3 shows the detailed specification of the balloon.

Table 3: PAWAN 1200 balloon specifications

| Specifications | Descriptions |
| --- | --- |
| Weight | 1200 g |
| Payload | 1000 g |
| Recommend Free Lift | 1180 g |
| Nozzle Lift | 2230 g |
| Gross Lift | 3430 g |
| Diameter at Release | 1.87 m |
| Rate of Ascent | 325 m/min. |
| Diameter at Burst | 0.80 m |
| Bursting Altitude | 30–32 km |
| Neck Diameter | 0.085 m |
| Neck Length | 20–22 cm |
| Color | Colorless/White |

The overall attachment configuration is shown in Figure 19. Notably, the attachment between the balloon and the parachute is separated by a 4 m-long paracord. This length reduces the frequency and amplitude of oscillations, thereby providing a less shaky video capture compared with short distance or direct attachment. The entire system consists of a balloon, a parachute, and a payload.
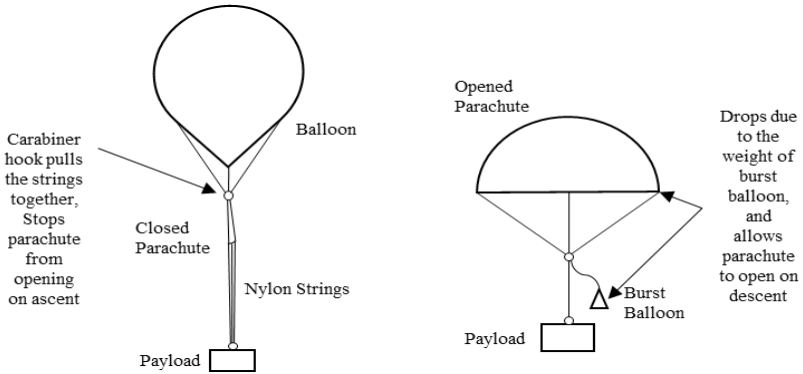
Figure 19: Configuration of balloon, parachute, and payload

## Final Design

The block diagram of the system and final design configuration of the HAB are shown in Figure 20 and
Figure *21*.
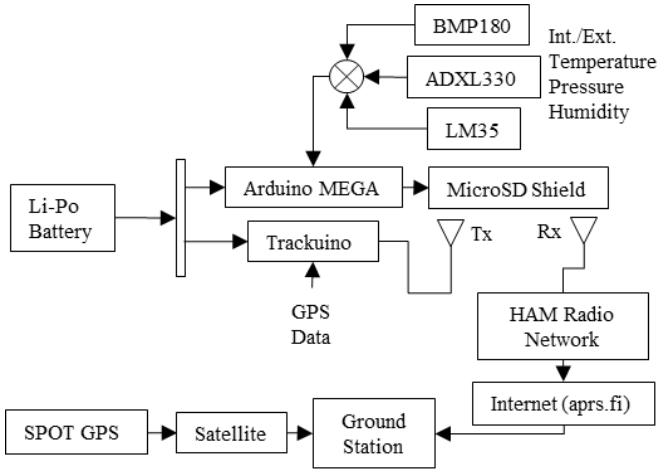
Figure 20: Block diagram of HAB payload component integration
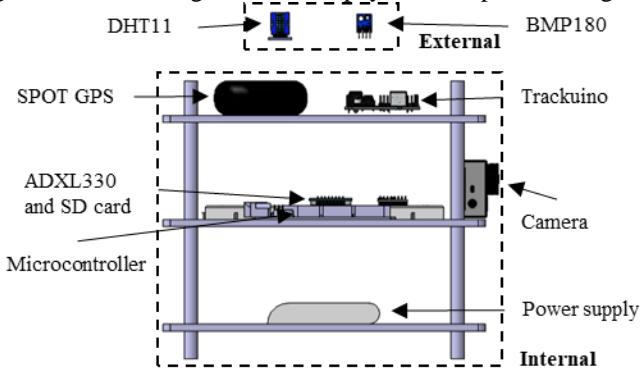


Figure 21: Front view of the HAB subsystem

## Launch Test

A launch flight test is conducted to test the system integration. The system comprises all the subsystems except Trackuino due to the unavailability to obtain the operating license. However, the only way to track the balloon is by use of SPOT Messenger GPS. This utilization is risky because the SPOT Messenger can only be used up until 6 km and that the GPS may lose connection in case the balloon floats away from the launch site. Nevertheless, the flight test is done successfully as the payload is retrieved. The data are then compared with the International Standard Atmosphere (ISA) data and from the Malaysia Meteorological Department (MET Malaysia).

## Atmospheric Data

Four atmospheric data are recorded during the flight test, which are altitude, temperature, pressure, and humidity. Figure 22 shows that the highest altitude recorded is 24.2 km. The maximum altitude is achieved at approximately 39 min. The total flight time is 1 h and 21 min, but the retrieval time takes the total mission time to nearly 3 h. The figure also shows that the ascent and descent rates are calculated as 9.2 and 10.4 ms$^{-1}$, respectively.

Figure 23 shows the temperature variation at different altitudes. The ISA data are obtained using Equations (4), (6), and (8) that are developed in 1920 by Toussaint [2]. The equations provide a simple and reasonable representation of the mean annual temperature results in United States although incomplete. Later in 1925, the standard atmosphere table is extended up to 20 km in altitude by Diehl. Diehl's standard atmosphere data are still used to date. However, the data are calculated only in United States at that particular time. The Standard Atmosphere Table is introduced as a reference atmosphere for the aviation industry, which requires some sort of average for calibrating altimeters, low-pressure chambers, and assessing the performance of aircraft under well-defined conditions. The Standard Atmosphere Table is not designed to be used in predicting the actual barometric pressure at a particular location. The table is developed by considering that latitude and seasons of the year can result in substantial local variations [18]. In [19], different months and different places are found to produce different temperature variations. Temperature changes with solar activity because a high correlation exists between solar activity and the Earth's surface temperature [20].
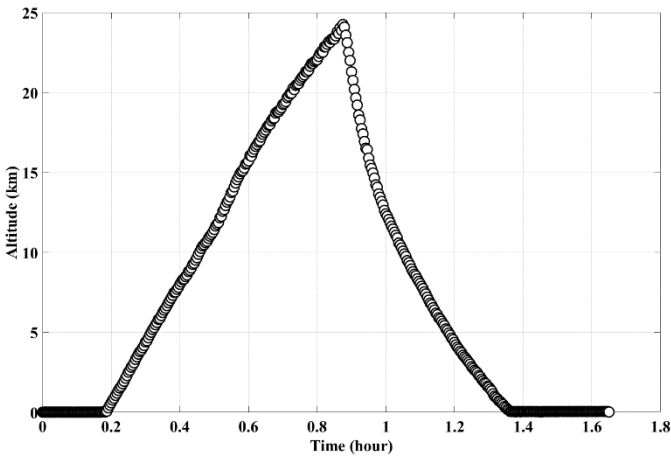


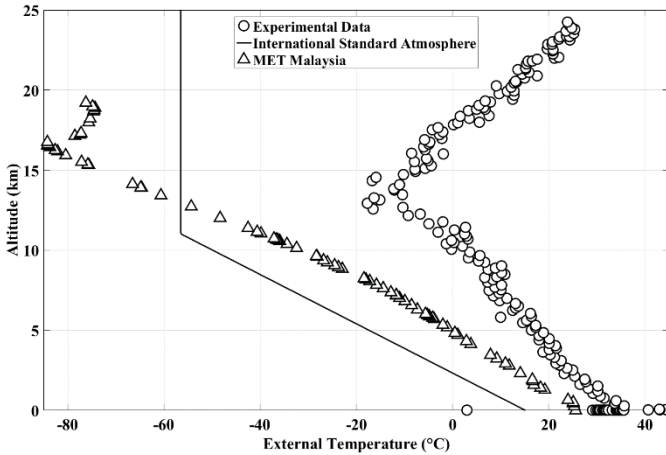Figure 22: Recorded altitudes during trial launch

Figure 23: Comparison of external temperature of payload bus with ISA data and MET Malaysia data at different altitudes

Figure 23 shows that the experimental data recorded by the BMP180 sensor is higher compared with the ISA and MET Malaysia data. This result is due to the placement of the BMP180 sensor that may be too close to the transmitter and the heat contained in the payload affecting the result. The data are still promising as the pattern is the same as the MET Malaysia data.

The data shown in Figure 24 indicate that the pressure recorded by the sensor is in accordance with the ISA and MET Malaysia data. The ISA data are determined using Equations(5),(7) and(9). Notably, the pressure decreases exponentially with recorded pressure of $0.158 \times 10^4$ N/m$^2$ at the maximum altitude.
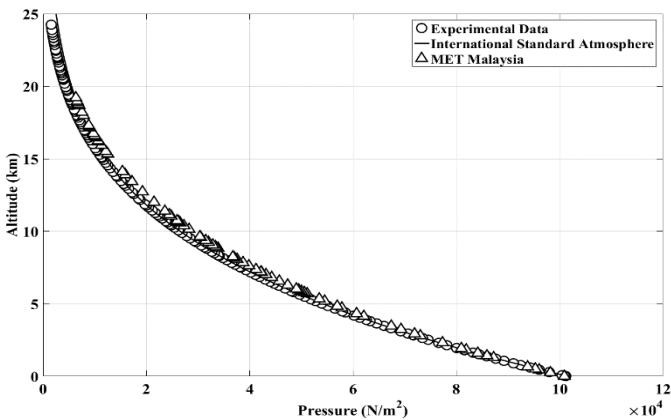
Figure 24: Comparison of pressure from experimental data with ISA data at different altitudes

Figure 25 shows the variation in humidity results compared with the data from MET Malaysia. The data from MET Malaysia are scattered but the pattern is the same as that of the experimental data in which the humidity reduces as the altitude increases. This condition is due to that the decrease in temperature results in cold air. The sensor works by measuring the temperature of the air as warm air will have high humidity content.
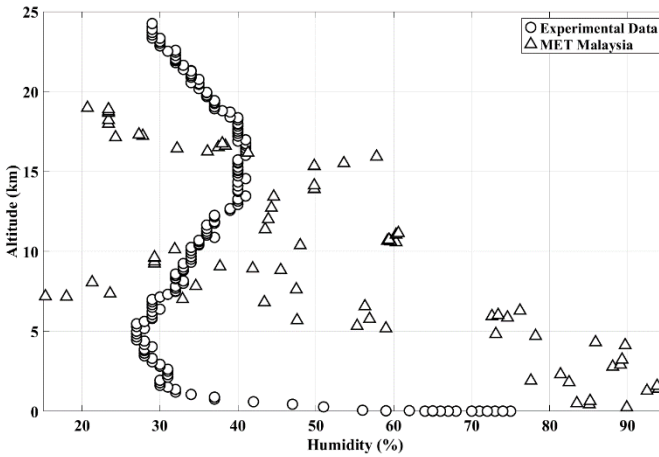


Figure 25: Variation in humidity data at different altitudes

## Balloon Trajectory

Prior to launching the HAB, the balloon trajectory is projected to estimate the landing position using the methods in [8] and [9]. Unfortunately, during the launch day, unavoidable circumstances delay the balloon release by 2 h. Hence, flight path prediction is performed again with new flight time as shown in Figure 26.

The prediction in Figure 26(a) shows the launch position, burst position, and balloon position. The flight time is predicted to be 2 h with a landing coordinate of 5°17'31"N, 99°28'14"E.
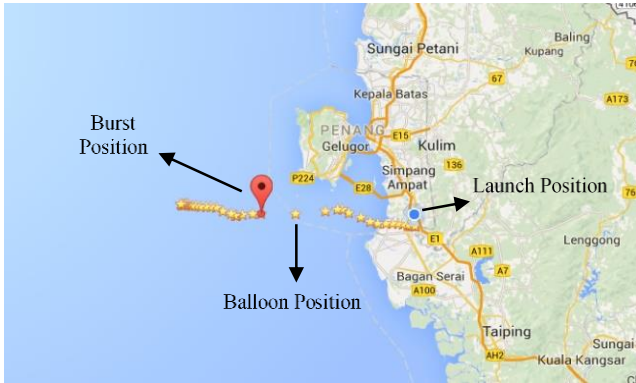
(a) Path tracking prediction result by Wyoming's predictor.
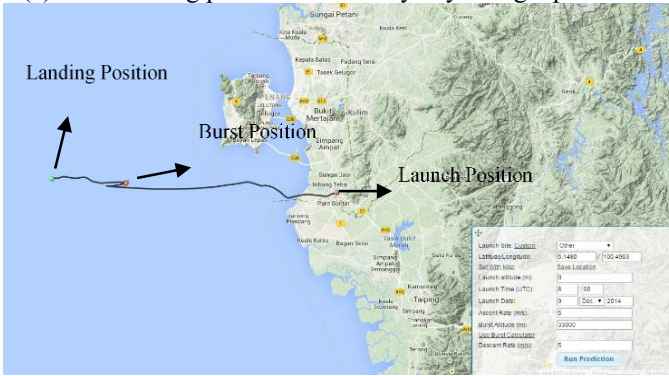


(b) Prediction using CUSF landing predictor

Figure 26: Prediction result from Wyoming and CUSF landing predictor

By using the CUSF landing predictor demonstrated in Figure 26(b), the total flight time is approximately 2 h compared with the Balloon Trajectory Forecasts by Wyoming University. The predicted landing position is at 5°17'31.3"N, 99°28'14.0"E, which is identical to the Wyoming's result. However, the location of landing position on both maps differs. However, Figure 27 shows that, with the distance of 0.83 km from point 1 (5°8'53.26"N, 100°29'44.83"E) to point 2 (5°8'35.82"N, 100°29'24.49"E), the latitude and longitude are approximately the same.

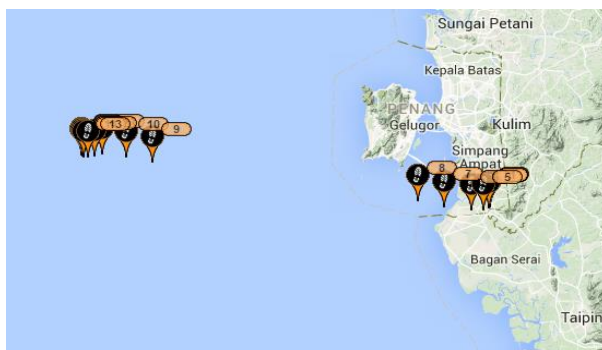Figure 27: Latitude and longitude measurement



Figure 28: Balloon trajectory recorded using SPOT Messenger during trial launch

Figure 28 shows the position recorded using SPOT Messenger. Notably, a large gap is found between position-feed 8 and position-feed 9. This gap is due to the commercial communication limit at the altitude of 6 km. Given that the commercial communication limit is at 6 km, the SPOT Messenger manages to keep running up until 24.2 km and sends signal back to the ground station when it reaches 6 km during descent. The landing coordinates registered by the SPOT Messenger is 5°17'31"N, 99°28'14"E. The flight path for all three tracking results is similar as shown in Figure 29. Therefore, the two predictors can provide an early estimation of the balloon trajectory but still fall short from the actual data as unknown assumptions are used during the software development. In addition, actual flight is affected by the unpredictable actual wind behavior.
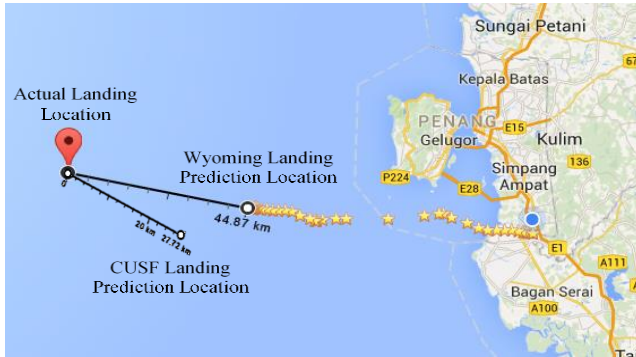
Figure 29: Comparison of landing position from the two predictors with actual landing position

## Image Results

Figure 30 shows the preparation and the actual launching of the HAB. Meanwhile,

Figure *31* shows several images taken during the flight, including the Earth's curvature.



<div align="center">(a)       (b)</div>

Figure 30: (a) Launch preparation of the HAB. (b) Launching of the HAB

(a) Earth's curvature at a maximum altitude of 24.2 km

Figure 31: Sample image of the Earth's curvature taken by the camera

## Conclusion

In this study, the mission analysis and hardware design for an HAB project are established by providing an insight on the working framework. The project is completed by undergoing component testing to test the reliability of each component, followed by integration testing. Each testing has its own case study. The system serves as a cost effective, near-space experiment platform for researchers. Apart from near-space experiments, this system can be employed in several situations, such as monitoring endangered species using thermal camera, sending supplies to flood or war victims, and controlling the parachute during landing. The HAB is experimentally launched to obtain a general idea on launching an HAB. This project also provides opportunity to test the components in actual condition. The result from the trial launch is successful as the data recorded are identical to the actual data.

## Acknowledgment

## References

[1]     P. Voss, (2009), "Advances in Controlled Meteorological (CMET) Balloon Systems," in *AIAA Balloon Systems Conference, 53(5), 1689–1699.*

[2]     J. D. Anderson Jr., (1999), "Aircraft Performance and Design", 1st ed. Boston: WCB/McGraw-Hill.

[3]     S. a. I. Mognet, T. Aramaki, N. Bando, et al., (2014), "The prototype GAPS (pGAPS) experiment," *Nuclear Instruments and Methods in Physics Research Section A: Accelerators, Spectrometers, Detectors and Associated Equipment,* 735, 24–38.

[4]     G. Osteria, and V. Scotti, (2013), "Euso-Balloon: A pathfinder mission for the JEM-EUSO experiment," *Nuclear Instruments and Methods in Physics Research Section* A: Accelerators, Spectrometers, Detectors and Associated Equipment, 732, 320–324.

[5]     J. Renard, G. Berthet, V. Catoire, et al., (2009), "Cobrat Project: Long Duration Balloons for the Study of High Energy Phenomena and Consequence for Stratospheric Chemistry," in *Proceedings of the 19th ESA Symposium on European Rocket and Balloon Programmes and Related Research*, 7-11 June 2009, (671), 181–186.

[6]     S. Katikala, (2014), "Google$^{TM}$ Project Loon," *Rivier Academic Journal,* 10(2), 3–8.

[7]     World View, "The World View Experience." [Online]. Available: *http://worldview.space/voyage/.* [Accessed: 25-Sep-2015].

[8]     University of Cambridge, "Cambridge University Spaceflight (CUSF) Landing Prediction." [Online]. Available: *http://predict.habhub.org/.* [Accessed: 20-Jun-2016].

[9]     University of Wyoming, "Balloon Trajectory Forecasts." [Online]. Available: *http://weather.uwyo.edu/polar/balloon_traj.html.* [Accessed: 20-Jun-2016].

[10]    T. G. Guzik, (2015), "The High Altitude Student Platform (HASP) as a model multi-payload balloon platform," in *2015 IEEE Aerospace Conference*, 1–10.

[11]    P. Techavijit, S. Chivapreecha, P. Sukchalerm, et al., (2016), "Suitable altitude for long-operated communication high altitude balloon with experimental flights," in *2016 8th International Conference on Knowledge and Smart Technology (KST)*, 169–174.

[12]    2010, "VHF Narrow Band FM High Power (300mW) Transmitter." [Online]. Available: *http://www.radiometrix.com/content/hx1.* [Accessed: 20-Jun-2016].

[13]    2016, "SPOT GPS Tracker." [Online]. Available: *http://www.findmespot.com/en/.* [Accessed: 20-Jun-2016].

[14]   P. Marian, 2014, "Arduino Uno Pinout." [Online]. Available: *http://www.electroschematics.com/7958/arduino-uno-pinout/.* *[Accessed: 20-Jun-2016].*

[15]   (2004), "Thermal Characteristics of Atmel Standard Package," San Jose, California.

[16]   J. D. Anderson Jr., (2000), "The Standard Atmosphere," in *Introduction to Flight, 4th ed., Boston*: WCB/McGraw-Hill, 766.

[17]   D. Poynter, (1991), "The Parachute Manual: A Technical Treatise on Aerodynamic Decelerators, Volume 1". *Para Publisher.*

[18]   J. B. West, (1996), "Prediction of barometric pressures at high altitudes with the use of model atmospheres," *American Physiological Society,* 1850–1854.

[19]   A. S. Jursa, (1985), "Handbook of Geophysics and The Space Environment", 1st ed. *Air Force Geophysics Laboratory, Air Force Systems Command, U.S. Air Force.*

[20]   X. ZHAO, and X. FENG, (2014), "Periodicities of solar activity and the surface temperature variation of the Earth and their correlations," *Chinese Science Bulletin (Chinese Version)*, 59(14), 1284.